Double photoemission studies at metal surfaces

N. Fominykh, J. Henk, J. Berakdar, P. Bruno

Max-Planck-Institut für Mikrostrukturphysik, Weinberg 2, D-06120 Halle (Saale), Germany

Abstract In the present work, we take a closer look at the theoretical model of double-electron photoemission (DPE) we have introduced in [1,2]. A local wave-vector-dependent approximation of the Coulomb interaction between the photoelectrons gives a connection of DPE to the one-step model of single photoemission (SPE). Calculations of DPE photocurrent for Cu(001) and Cu(111) surfaces are provided to illustrate the interplay between scattering and correlation, as well as the manifestation of the single-particle properties in angular and energy sharing distributions.

1. INTRODUCTION

In DPE the single photoabsorption event leads to the simultaneous emission of two photoelectrons. These are detected with energy and momentum resolution, the simultaneity of their creation is controlled by the time-of-flight technique [3]. To our knowledge, a theoretical investigation of DPE from surfaces has been undertaken in two different frameworks. In the first one [4], the DPE matrix element was evaluated for the jellium-like semi-infinite solid and screened Coulomb interaction between outgoing electrons. It was shown that there exists a certain condition for the diffraction of the correlated electron pair and a certain DPE selection rule. The second approach [1,2] was oriented towards utilization of the up-to-date level of single photoemission (SPE) calculations [5] in order to be able to use realistic surface band structures and densities of states. Accurate treatment of single-particle properties requires a manageable form of the interaction between the two photoelectrons. We designed a method in which the screened Coulomb potential was incorporated in a non-perturbative way into the one-particle Green's functions, provided by an *ab initio* SPE computer code [5]. The screening length λ is a parameter derived from a Thomas-Fermi approach. In this way the two-electron photocurrent can be approximately expressed through the one-particle matrix elements, formally resembling the ones encountered in one-step model of SPE (see e. g. [6]). Our first numerical results [2] revealed the fingerprints of the electronic correlation, in particular the appearance of Coulomb correlation hole, and confirmed the expected qualitative trends. In the present work we continue these investigations and calculate the DPE photocurrent from Cu(001) and Cu(111) surfaces. In Sec.2 we discuss DPE angular distributions (ADs), Sec.3 deals with energy sharing distributions (ESDs), Sec.4 summarises the results.

CP604, *Correlations, Polarization, and Ionization in Atomic Systems*
edited by D. H. Madison and M. Schulz

2. ANGULAR CORRELATION PLOTS

The experimentally defined two-electron final state provides six independent variables: four angles of emission $(\theta_1, \phi_1), (\theta_2, \phi_2)$ and two kinetic energies E_1, E_2 . Two particular situations will be considered here. At a given energy and (linear) polarization of the photon the DPE probability will be given: (i) as a function of the energy difference $(E_1 - E_2)$ at fixed total energy $E_{tot} = E_1 + E_2$ and fixed angles (θ_1, ϕ_1), (θ_2, ϕ_2), or (ii) as a function of (θ_2, ϕ_2) for fixed (θ_1, ϕ_1) and E_1, E_2. The first mode is referred to as energy sharing distribution (ESD), the second one is the DPE angular distribution (AD).

The scattering of the electrons from the lattice and their mutual repulsion most easily can be observed in the DPE ADs. In general, the DPE intensity depends on the difference in emission angles according to two competing tendencies. This angle should be small enough to provide sufficient interaction, and it should be large enough to avoid strong Coulomb repulsion. Therefore the region of high DPE intensity looks roughly like a 'ring' around the fixed-electron direction (see Fig.1 and it's caption). This general pattern is mixed with the diffraction effects due to scattering of the electrons from the lattice. The mean angle with respect to the first electron, at which the second electron is preferrentially emitted, depends on the value of the screening length λ and, hence, on the material. For the lack of space we are not visualizing this trend here: The larger is

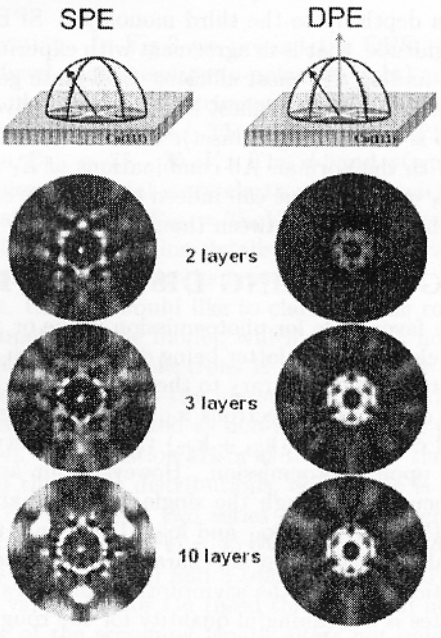

Figure 1 DPE ADs from Cu(111) surface (right column) in the form of stereographic projection. The direction of emission of the 'fixed' electron is perpendicular to the surface, as shown by a grey arrow on the sketch above. $\hbar\omega = 45\ eV$, $E_1 = E_2 = 15\ eV$, the light is polarized normally to the surface. For comparison, the left column shows the SPE ADs. The normalized intensity from zero to one is shown by black-and-white scale (the normalization is the same within each column and differs by five orders between the columns). The angle of emission, which is varied, is shown by a black arrow in both sketches.

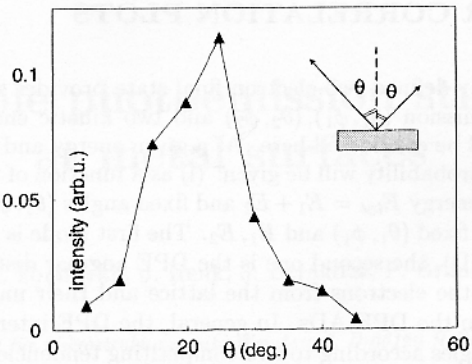

Figure 2 Cu(001) DPE intensity, averaged over all possible energy sharings between photoelectrons for given ω and E_{tot}. $E_{tot} = 33\,eV$, $\omega = 45\,eV$, angle θ changes simultaneously for both electrons and serves as an abscissa of the plot. Here and below angles ϕ_1, ϕ_2 are set to zero.

the region where the electrons can interact and decline their trajectories, the wider will be the 'ring' of high intensity. The depth of generation of correlated pairs, as compared to the depth of generation of photoelectrons in SPE process, is illustrated by showing the photocurrents from 2, 3 and 10 monolayers of Cu(111). One can see that most of the DPE signal is formed at a depth up to the third monolayer. SPE and DPE intensities differ by five orders of magnitude, that is in agreement with experimental observation. In Fig.2 we are interested in finding the 'most efficient' final state geometry, i.e. the angle between two electrons, which gives the highest DPE rate at a given photon energy and E_{tot}. The following set up is chosen (Fig.2, inset): electrons are directed symmetrically, each making an angle θ with the normal. All combinations of E_1 and E_2 are taken into account, which satisfy $E_{tot} = 33\,eV$. One can indeed observe the single peak of intensity at $\theta = 25^0$ as a result of the interplay between the above trends.

3. DPE ENERGY SHARING DISTRIBUTIONS

An ESD shows, how favourable for photoemission is one or another *sharing* of the total energy between two electrons, the latter being dependent on the momentum transfer due to the Coulomb interaction. Contrary to the SPE process, in DPE the individual surface-parallel momenta of the photoelectrons $\mathbf{k}_{\|1,2}$ are, in general, not conserved. It is the sum of the parallel components $(\mathbf{k}_{\|1} + \mathbf{k}_{\|2})$ that is conserved (*modulo* a surface reciprocal lattice vector) upon photoemission. However, our approximate expression of the two-electron photocurrent through the single-particle matrix elements [1,2] implies the conservation of the individual $\mathbf{k}_{\|1}$ and $\mathbf{k}_{\|2}$. Thus, only those initial states are participating in the optical transition, that are characterized by the same irreducible representation of the translation group as the asymptotic final states. This means that the $\mathbf{k}_{\|}$-resolved density of states is a meaningful quantity for the rough analysis of the DPE ESDs. Finally, being the optically excited flux, ESD reflects the features of the dipole transition and contains a kinematical factor $\sqrt{E_1 \cdot E_2}$ (in the non-relativistic case). The latter explains the zero value of the ESD at the edges, where either E_1 or E_2 is equal to zero. So, each point of the ESD is related to certain E_1, E_2 and corresponding $\mathbf{k}_{\|}$-resolved densities of initial states. This relation is not straightforward, since one has to integrate the DPE current over a certain energy range of the initial states [2], as defined

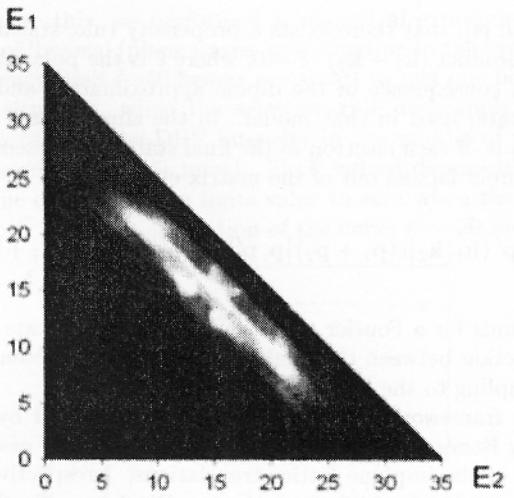

Figure 3 DPE intensity (black-and-white contrast) as a function of E_1, E_2. Electrons are emitted at 30^0 symmetrically with respect to the surface normal. The photon energy $\omega = 45\,eV$ and the Fermi energy $E_F \sim 5\,eV$ define the maximal total energy $E_{tot} \sim 35\,eV$.

by the energy conservation. In Fig.3 we present the DPE current from Cu(001) as a function of E_1, E_2 for fixed photon energy (p-polarized light) and fixed angles of emission. The difference of this plot and the experimental ones (see example in [3]) is due to the disregard of the secondary processes. The appreciable DPE signal (white region) is obtained in the region $E_{tot} = 25 \ldots 35\,eV$. The d-band of copper ($\sim$3 eV band below the Fermi level) supplies the initial state electrons; pairs with $E_{tot} < 25\,eV$ and in the narrow black band just below the $E_{tot} = 35\,eV$ boundary are not accessible due to the low density of the initial states. Fine details on the picture arise from the Coulomb interaction and multiple scattering at the crystal potential.

The next aspect, that we would like to clarify, is the role of the screening length λ. It is the only parameter in the model, which describes how effectively the range of interaction between two outgoing electrons is *cut-off* by the ground state electrons of the surface. The screening length is the measure of the interaction, for if it is strongly screened, the electrons may be treated as non-interacting, in which case the DPE probability becomes zero [4]. The question arises as to whether the screening length changes only the magnitude of the ESDs distributions, or it's role is dynamical, i.e. influences their shapes too. In Fig.4 we plot two series of ESDs, where both trends are shown. Fig.4(a) corresponds to E_{tot}=33 eV, $\omega = 45$ eV, $\theta_1 = -\theta_2 = 20^0$, $\lambda = 1.0, 2.66, 4.0\,a_0$ for the curves 1 (long-dashed), 2 (solid) and 3 (dashed), respectively. Curve 2 corresponds to the Thomas-Fermi value of λ for Cu (used throughout if not stated otherwise). One can see that the value of the screening length alters not only the magnitude, but also the shape of ESD. In Fig.4(b) the values of λ and the geometry are the same except for the angles of emission: $\theta_1 = -\theta_2 = 40^0$. It may be inferred, that for the larger angle between electrons the ESD shapes are less sensitive to screening and the role of the screening length is only scaling.

It was shown in [4], that there exists a propensity rule, stating that DPE current is zero if the scalar product $(\mathbf{k}_1 + \mathbf{k}_2) \cdot \hat{\epsilon} = 0$, where $\hat{\epsilon}$ is the polarization vector of light. It was deduced as a consequence of the dipole approximation and the approximation for the DPE final state, used in that model. In the simple case, whatever the initial two-particle state Φ_2 is, if each electron in the final state is represented by a plane wave, the above scalar product factors out of the matrix element:

$$M_{\mathbf{k}_1,\mathbf{k}_2} = \int \mathrm{d}^3\mathbf{p}\,\mathrm{d}^3\mathbf{p}' \left\langle \mathbf{k}_1, \mathbf{k}_2 \middle| \hat{\epsilon}(\mathbf{p}_1 + \mathbf{p}_2) \middle| \mathbf{p}, \mathbf{p}' \right\rangle \left\langle \mathbf{p}, \mathbf{p}' \middle| \Phi_2 \right\rangle = \hat{\epsilon}(\mathbf{k}_1 + \mathbf{k}_2) \cdot \tilde{\Phi}_2(\mathbf{k}_1, \mathbf{k}_2) \ , \quad (1)$$

where $\tilde{\Phi}_2(\mathbf{k}_1, \mathbf{k}_2)$ stands for a Fourier transform of the initial state. This remains valid also when the interaction between the final state electrons is present, but disregarded is the final-channel coupling to the host system.

In the present framework the final states are represented by the so-called time-reversed LEED (Low Energy Electron Diffraction) states, whose essential feature is that they are eigenstates of the in-plane lattice translations. Irrespective of the form of the initial state, the matrix element built from the two Bloch sums in the final state reads:

$$M_{\mathbf{k}_1,\mathbf{k}_2} = \int \left\langle \sum_{\mathbf{g}} a_{\mathbf{g}} \mathrm{e}^{-\mathrm{i}(\mathbf{k}_1+\mathbf{g})\mathbf{r}} \cdot \sum_{\mathbf{g}'} b_{\mathbf{g}'} \mathrm{e}^{-\mathrm{i}(\mathbf{k}_2+\mathbf{g}')\mathbf{r}'} \middle| \hat{\epsilon} \cdot (\mathbf{p}_1 + \mathbf{p}_2) \middle| \mathbf{p}, \mathbf{p}' \right\rangle \times$$

$$\times \ \left\langle \mathbf{p}, \mathbf{p}' \middle| \Phi_2 \right\rangle \mathrm{d}^3\mathbf{p}\,\mathrm{d}^3\mathbf{p}' = \tilde{\Phi}_2(\mathbf{k}_1, \mathbf{k}_2) \cdot \sum_{\mathbf{g}\,\mathbf{g}'} a_{\mathbf{g}} b_{\mathbf{g}'}\ \hat{\epsilon} \cdot (\mathbf{k}_1 + \mathbf{k}_2 + \mathbf{g} + \mathbf{g}'). \quad (2)$$

Here $a_{\mathbf{g}}$ and $b_{\mathbf{g}'}$ are the coefficients in the Bloch expansion of the LEED states, vectors $\mathbf{g}$ and $\mathbf{g}'$ are the (surface) reciprocal lattice vectors. In general, the last sum in Eq.(2) cannot be zero for any choice of $\mathbf{k}_1$, $\mathbf{k}_2$, $\hat{\epsilon}$, and the selection rule described before does not hold. On the other hand, the plane-wave representation of the LEED state becomes adequate when going to higher kinetic energies, meaning that the selection rule becomes

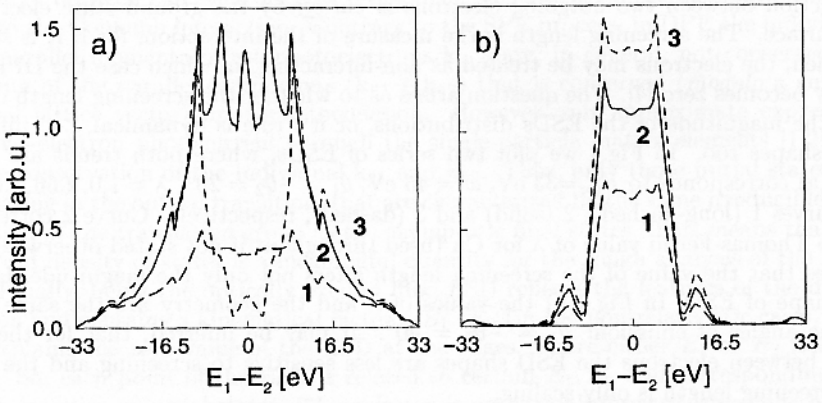

Figure 4 DPE EDS from Cu(001) for different values of the screening length (see text for details).

applicable. To estimate this, we performed a 'numerical experiment', deliberately decreasing the number of 'beams' (plane waves, participating in the expansion of the LEED states) from convergency limit (~40 beams per state) to just one beam. The latter case would simulate the situation, when the selection rule does apply. The value, which should vanish in this case, is the DPE intensity in the middle of the ESD ($E_1 = E_2$) for the symmetric geometry (Fig.5, inset). Fig.5 indeed demonstrates the downfall of the middle-point value of ESD from a finite value to zero when the number of beams is decreased from 37 to 1. Note the saturation of the curve at ~20 beams per state.

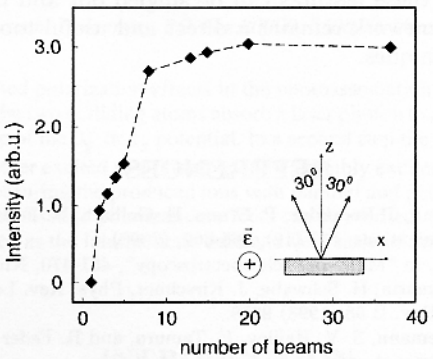

Figure 5 Cu(001) DPE current at $E_1 = E_2 = 15\,eV$, $\omega = 45\,eV$, $\theta_1 = -\theta_2 = 30^0$, $\hat{\epsilon}$ parallel to y-axis, calculated for different number of plane waves in the expansion of the LEED states.

This conclusion is supported by another setup, Fig.6, in which ω and E_{tot} are concurrently growing. The value of the ESD at $E_1 = E_2$ is maximum at E_{tot}=13 eV and decreases towards higher energies. The variety of ESD shapes in Fig.6 is guided by several factors: (i) the interaction between electrons depends on their kinetic energies; (ii) the Bloch spectral functions of the initial states are 'scanned' differently along different ESDs; (iii) the number of relevant 'beams' changes with energy.

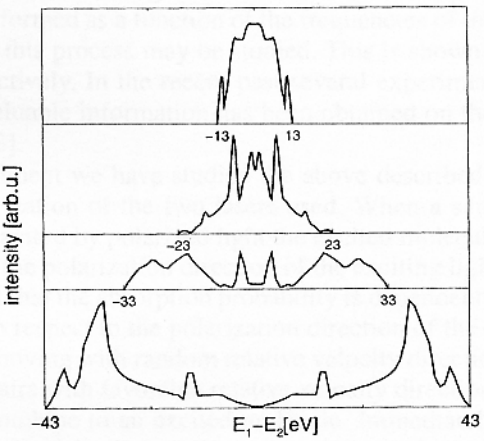

Figure 6 ESDs from Cu(001) for ω=25, 35, 45 and 55 eV and E_{tot}=13, 23, 33 and 43 eV, respectively. For all cases the ejection angles are $\theta_1 = -\theta_2 = 30^0$, $\hat{\epsilon}$ parallel to x-axis.

4. SUMMARY

We have presented numerical results of DPE calculations from copper surface. Some of them, like the manifestation of Coulomb interaction in the angular distribution of the DPE cross section, can be understood from simple qualitative reasoning. Another, like the role of initial state densities, the screening and the non-plane-wave character of the electronic states are not obvious, have a strong effect on the DPE spectra and require extensive numerical investigations. The analysis of the DPE distributions is complicated by the fact that none of these features can be singled out and traced separately. Nevertheless, the present framework remains a direct and useful tool for the exploration of correlation-accented techniques.

REFERENCES

1. N. Fominykh, J. Henk, J. Berakdar, P. Bruno, H. Gollisch, R. Feder, Solid State Communications, 113 (12), 665-669, (2000)
2. N. Fominykh et. al., in "Many-particle spectroscopy", 461-470, Kluwer (2001).
3. R. Herrmann, S. Samarin, H. Schwabe, J. Kirschner, Phys. Rev. Lett. 81 (1998) 2148.
4. J. Berakdar, Phys. Rev. B 58 (1998) 9808.
5. J. Henk, T. Scheunemann, S. V. Halilov, E. Tamura, and R. Feder (1999) *omni* – fully relativistic electron spectroscopy calculations.
6. S. V. Kevan (ed.), Angle-resolved Photoemission, Elsevier, Amsterdam (1992).